Methane in carbon nanotube - molecular dynamics simulation

Katarzyna Bartuś, Aleksander Bródka

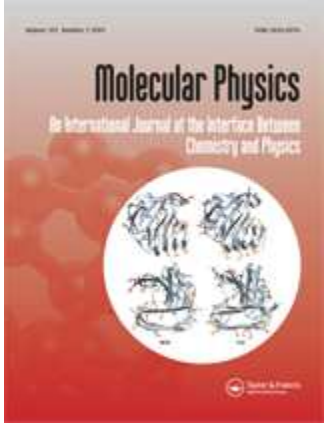

Methane in carbon nanotube – molecular dynamics simulation

Journal:	*Molecular Physics*
Manuscript ID:	TMPH-2010-0490.R2
Manuscript Type:	Full Paper
Date Submitted by the Author:	21-Apr-2011
Complete List of Authors:	Bartuś, Katarzyna; University of Silesia, A. Chełkowski Institute of Physics Bródka, Aleksander; University of Silesia, A. Chełkowski Institute of Physics
Keywords:	MD simulations, methane molecule in carbon nanotube

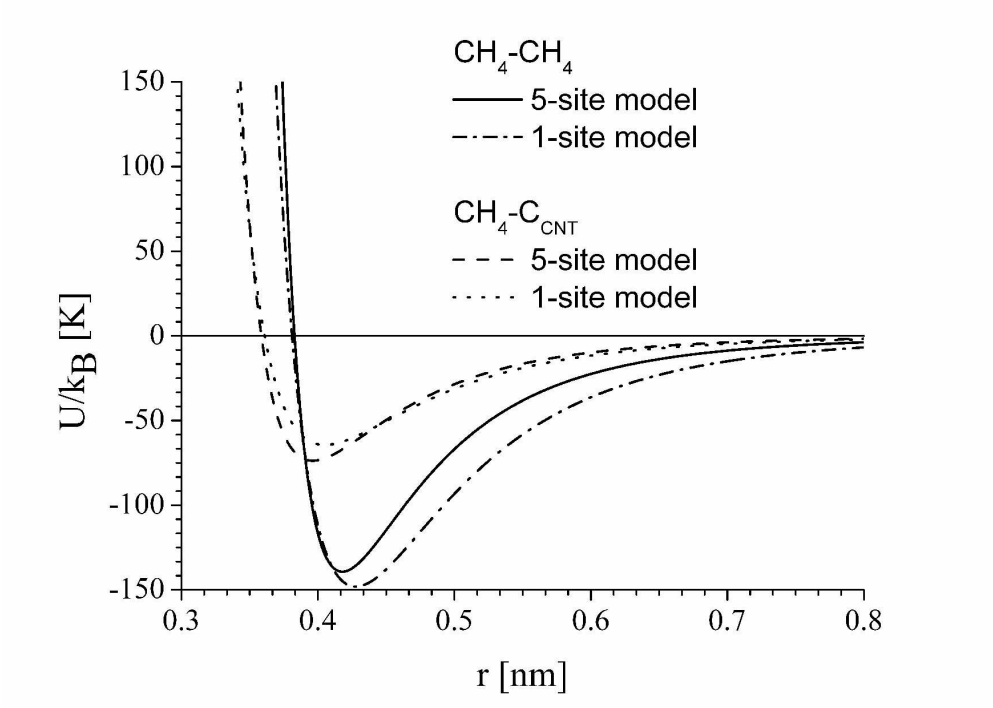

1188x839mm (150 x 150 DPI)

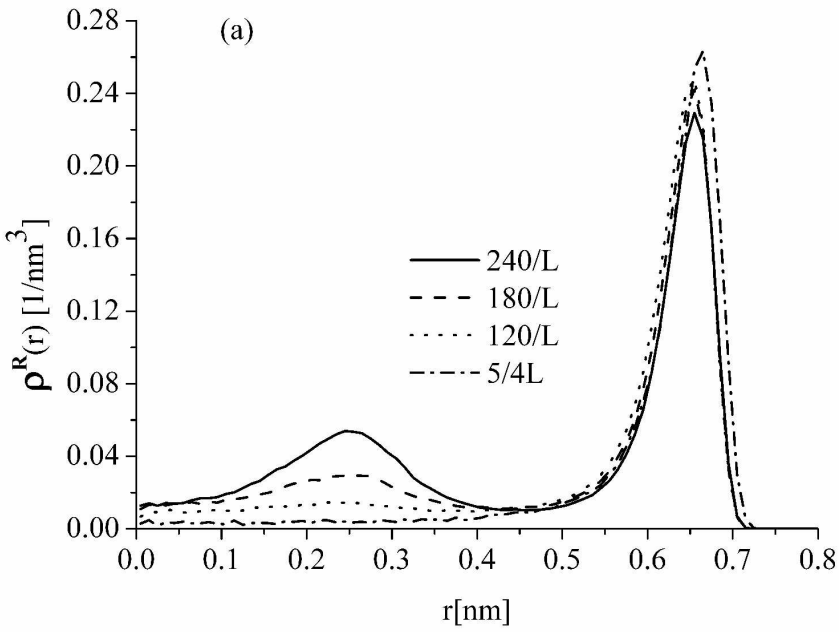

1188x839mm (150 x 150 DPI)

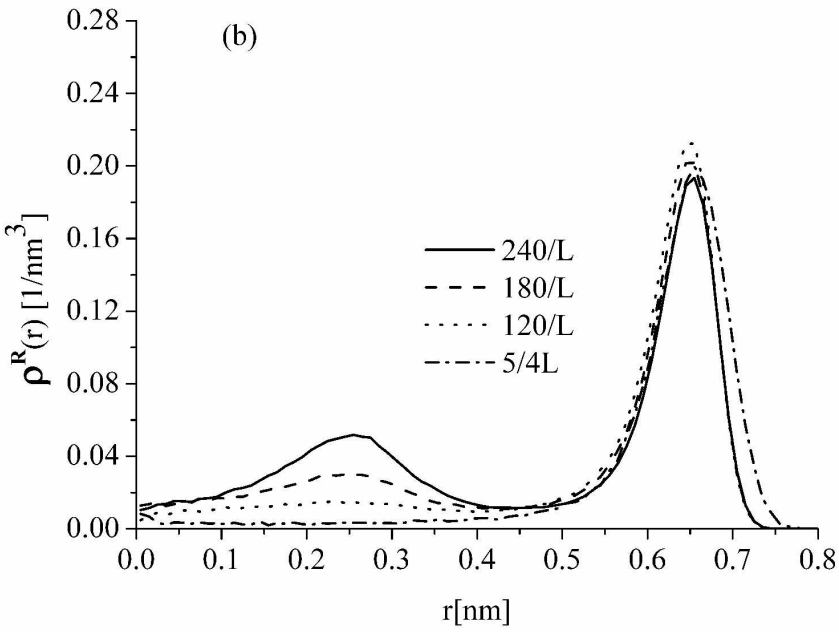

1188x839mm (150 x 150 DPI)

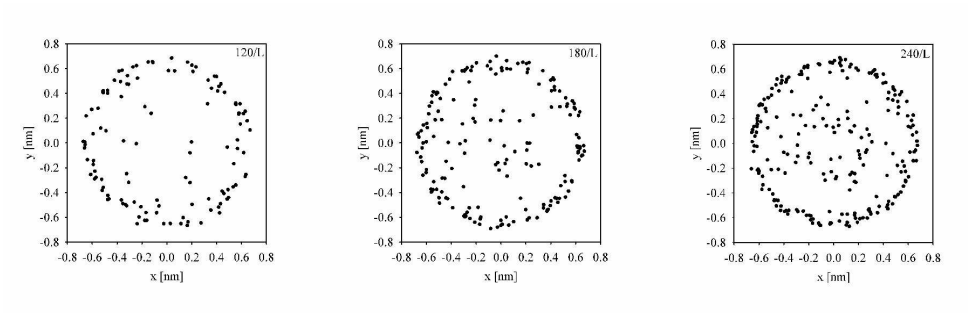

1255x391mm (150 x 150 DPI)

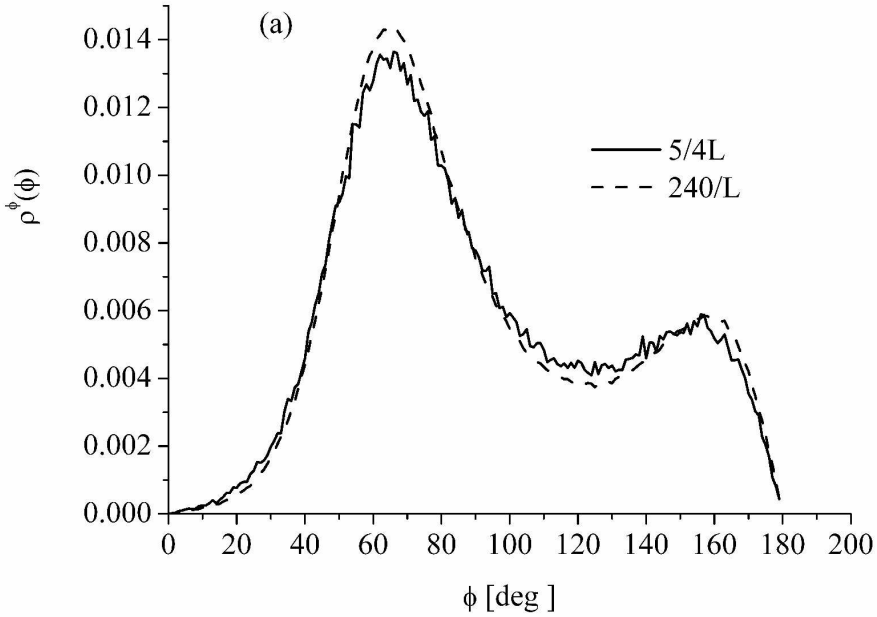

1188x839mm (150 x 150 DPI)

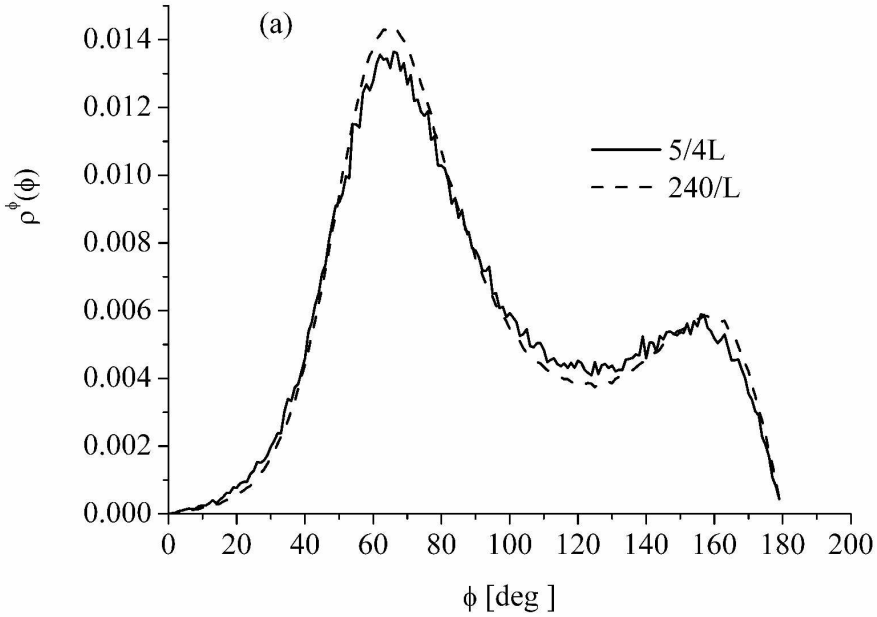

1188x839mm (150 x 150 DPI)

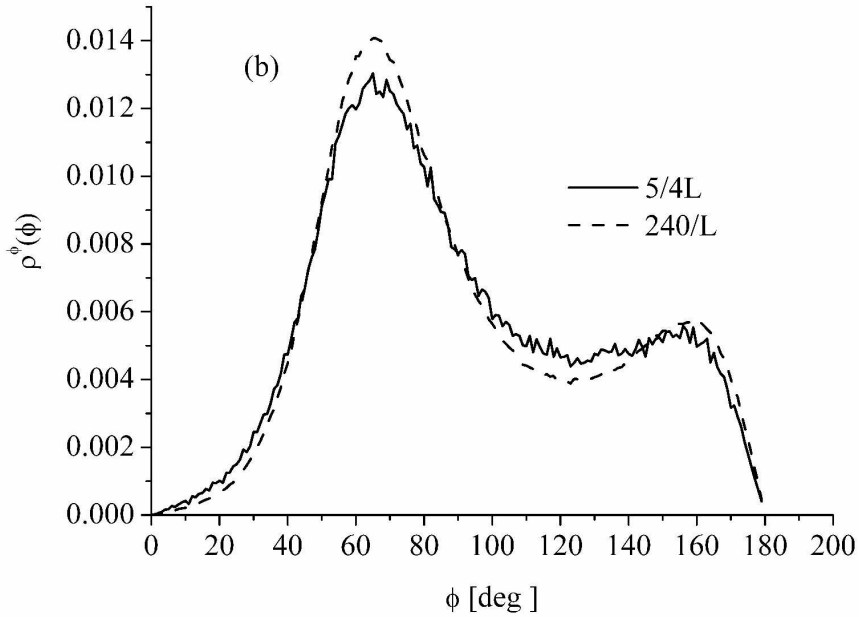

1188x839mm (150 x 150 DPI)

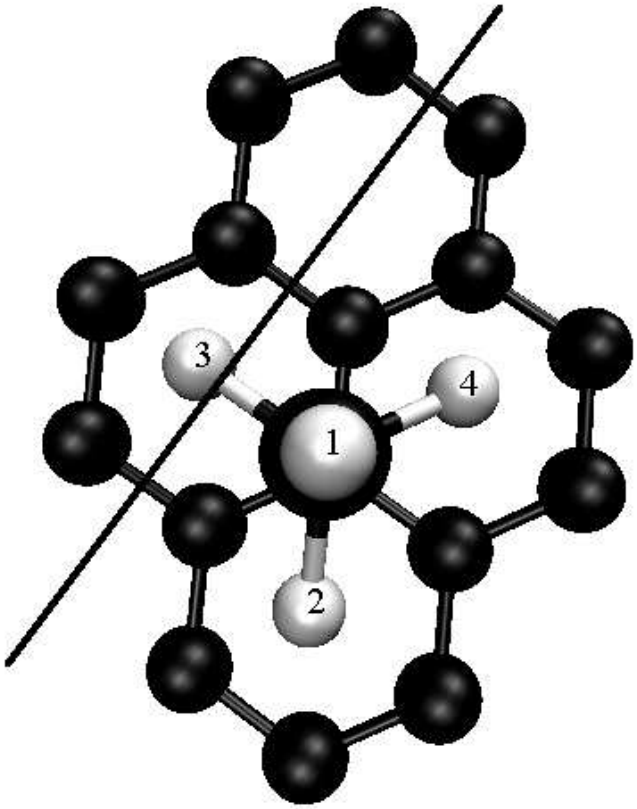
3
4
1
2

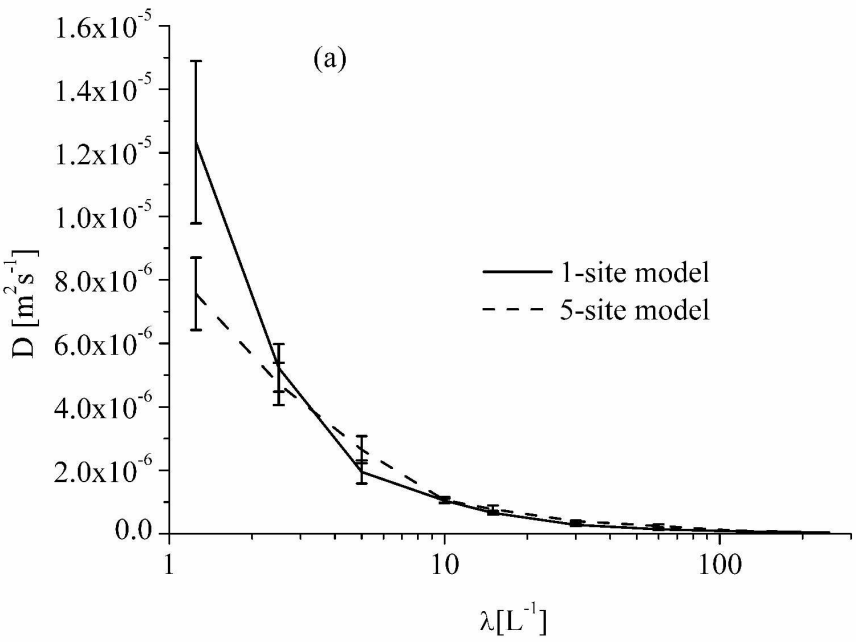

1188x839mm (150 x 150 DPI)

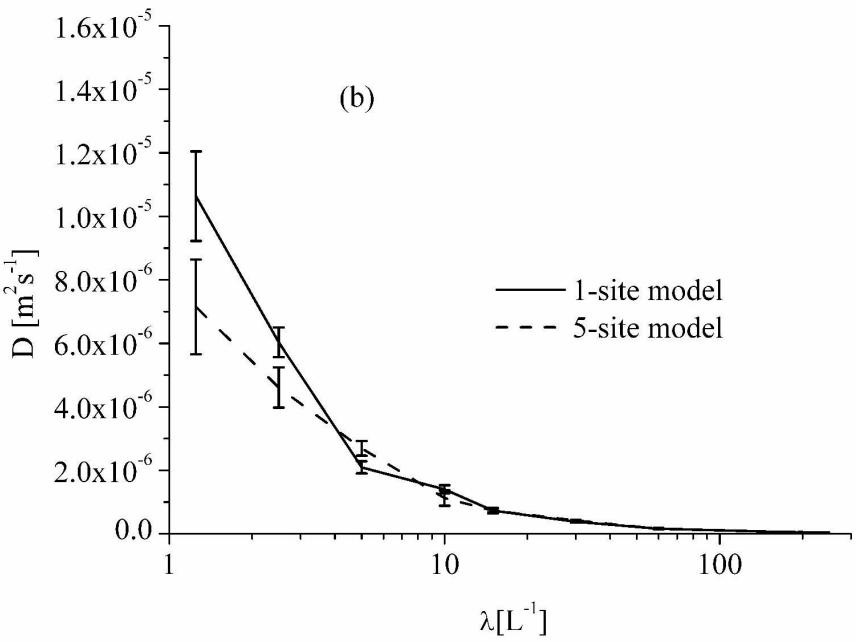

1188x839mm (150 x 150 DPI)

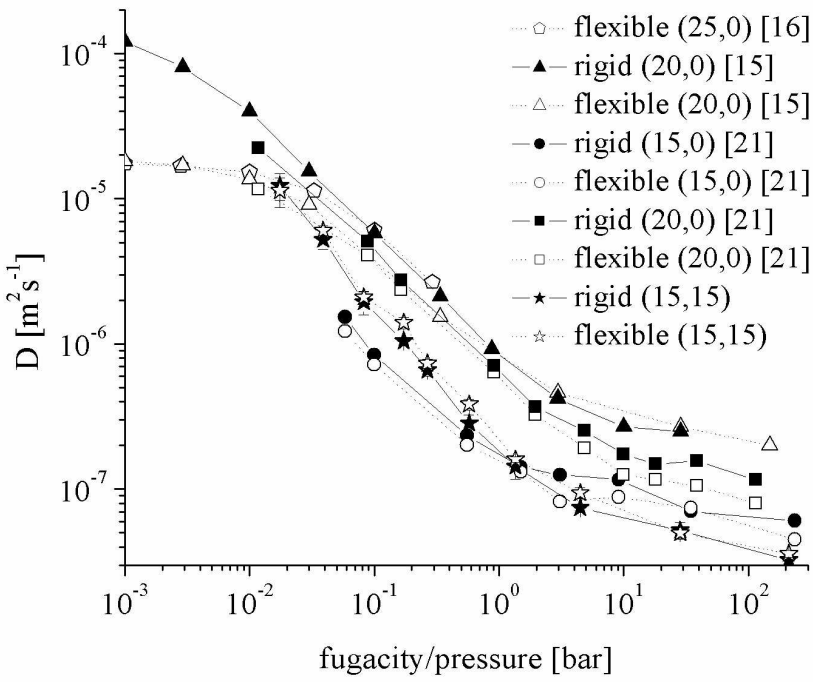

279x215mm (150 x 150 DPI)

Methane in carbon nanotube – molecular dynamics simulation

Katarzyna Bartuś and Aleksander Bródka

A. Chełkowski Institute of Physics, University of Silesia, Uniwersytecka 4, 40-007 Katowice, Poland

The behaviour of methane molecules inside carbon nanotube at room temperature is studied using classical molecular dynamics simulations. A methane molecule is represented either by a shapeless super-atom or by rigid set of 5 interaction centres localised on atoms. Different loadings of methane molecules ranging from the dense gas density to the liquid density, and the influence of flexibility of the CNT on structural and dynamic properties of confined molecules are considered. The simulation results show the decreases of the diffusion coefficient of methane molecules with density. At higher densities diffusion coefficient values are almost independent of molecular shape, but at low densities one observes faster motion of the super-atom molecule than that for the tetrahedral model of the molecule. For loadings of methane considered here the nanotube flexibility, introduced by the reactive empirical bond order (REBO) potential for interactions between carbon atoms of nanotube, does not have effect on diffusivity of methane molecules, and its impact on the molecular structure is weak. It is found that methane molecules in the vicinity of the nanotube wall show tripod orientation with respect to the nanotube surface.

Keywords: diffusion; carbon nanotube; methane molecule

1.Introduction

In last years carbon nanotubes (CNTs) have been subjected to intensive research because of their excellent combinations of mechanical, electrical and chemical properties. Furthermore, because of their nanometer-scale size, cylindrical shape, uniform porosity and high tensile strength CNTs have many potential applications such as molecular sieves, ultrafiltration membranes [1], sensors [2] and nanometer-sized pipes for the precise delivery of gases and liquids [3]. It is also of practical interest in connection with gas separation and purification, the development of storage media for natural gas and the behaviour of methane in underground reservoirs. The dynamics of fluids and gases in systems with restricted geometry is known to be very different from that in the bulk phase. Attempts to understand, and hence control the transport properties are well motivated by fundamental and applied

interests. Recently, adsorption of methane in CNTs [4-7] and on them [8-13] have been studied experimentally. To investigate behaviour of methane inside CNTs molecular dynamics (MD) simulations [14-27] and Monte Carlo (MC) ones [28-32] have been used, however, in most of the studies the CH_4 molecule was represented by a spherical super-atom, i.e. the 1-site model, and only few of them modelled the methane molecule by 5 interaction centres, i.e. the 5-site model [18,25-27]. For 1-site model molecular simulations of rigid CNT have shown that the diffusion coefficient decreases with the increase of adsorbate concentration [15-17,21]. The diffusion coefficient of methane molecules in a rigid (10,10) CNT drops rapidly from value about $1\cdot10^{-4}$ m^2/s in the limit of low concentration to about 10^{-7} m^2/s at high pore loadings [17]. In the limit of low density, diffusion coefficient of methane in the (20,0) CNT at room temperature was about $0.2\cdot10^{-4}$ m^2/s in flexible nanotube, whereas in a rigid one it was about $1.2\cdot10^{-4}$ m^2/s [15]. It means, that at the lowest density flexibility of the CNT reduces the diffusion coefficient of methane molecules approximately by a factor of 6. For nondilute pore loadings, the difference between behaviour of methane in the rigid nanotube and flexible one is very small, and for loadings resulting in pressures greater than 0.1 bar the nanotube flexibility seems to be meaningless. For the 5-site model of CH_4 in rigid nanotubes of various diameters and helical structure were considered in the MD simmulations performed at 300K for different densities of methane molecules inside CNT [18,25,26], but influence of flexibility of CNT on the behaviour of the CH_4 molecules was not studied. MD simulations of liquid methane with densities from 0.353 to 0.17 g/cm^3, confined in CNTs with diameters 0.7-1.4nm [18,25,26] showed that flow of methane does not depend on the helicity of the CNT but it depends on the tube diameter. For motion of methane molecules along the CNT the simulations predict normal-mode diffusion, i.e. the mean square displacement function is proportional to time [18,25-27]. The MD simulation results gaves also possibility to estimate the distance between CH_4 molecule and inner wall of CNT, and for the (10,0) CNT the distance was 0.3nm and for the (10,10) one it was 0.35nm [25]. Whcich is in accordance with the distance 0.348 nm obtained for the 1-site model of CH_4 molecules in the rigid (10,10) CNT [24]. Adsorption of methane molecules on the CNT surfaces was also studied using density functional theory (DFT) method [33-38] and second order Möller-Plesset perturbation calculations [39]. Usually the studies considered few methane molecules and CNTs with small diameters, and concentrated on binding energies of adsorbed molecules and their positions with respect to the CNT.

A single wall CNT can be formed from a graphene sheet, and hence the nanotube surface is closely related to that of graphite, which is considered as standard substrate in experimental studies of 2D adsorbed phases [40-46] as well as theoretical ones [41,47-55]. Therefore, results of studies of methane on graphite can be helpfull in understending behaviour of methane molecules in CNTs. Moreover, those studies were used to determine parameters of the interaction potential between CH_4 molecule and carbon atoms of graphene sheet [56].

In this paper we present results of MD simulations of methane inside the (15,15) CNT for two models of the CH_4 molecule are used: a usually applied united atom and tetrahedral model taking into account atom positions in the molecule. We analyze the influence of molecular model on structure and dynamics of the system. The MD simulations were carried out for different loadings of methane in the CNT. We consider densities lower than those for liquid methane used previously [18,24]. Distribution of methane molecules and their orientations in the CNT are investigated and self-diffusion coefficient values are estimated using the mean square displacements as well as velocity correlation functions. Moreover, to study impact of flexibility of the CNT on behaviour of the confined methane we consider rigid and elastic model of the nanotube.

2. Computational Details

We performed the MD simulations of methane in single-walled (15,15) CNT with diameter d=2.034 nm and length L=11.068 nm. The CNT was generated using two-dimensional perfectly hexagonal graphene sheet with the carbon-carbon bond length of 0.142 nm, and the sheet was wrapped into seamless cylinder. To simulate different loadings, we usually change the number of methane molecules, however, to obtain low densities we increase length of the CNT two or four times, and systems considered here are defined in Table 1. Assuming smooth wall of the nanotube we estimated densities of methane inside the CNT, which are in the range from 0.178 g/cm^3 to 0.9 mg/cm^3. The density estimated for the smallest system is larger than the density of methane at room temperature and ambient pressure. For each system size the MD simulations are performed for two models of CNT: rigid where carbon atoms are frozen and flexible, in which the carbon atoms undergo thermal motions resulting from interactions with atoms of the CNT and methane molecules. Interatomic interactions of carbon atoms in flexible CNT are described by REBO potential [57], which was originally parameterized to examine

the growth of diamond thin films by chemical vapour deposition. The REBO potential has also been successfully used to study the structure of carbon nanotubes [58] and their mechanical properties [59,60]. Moreover, the interaction potential was used to investigate structural properties of activated carbons [61] as well as nanodiamonds and carbon onions [62]. We considered two models of the CH_4 molecule. The first is the usually applied the 1-site model [14-17,19-24], and the second one called the 5-site model is a rigid tetrahedron with a central carbon atom and four hydrogen atoms [56]. Intermolecular interactions are modelled by Lennard-Jones (LJ) potential, and its parameters for both models are collected in Table 2. For the 1-site model the LJ potential parameters for unlike interacting centres presented in Table 2 were calculated using the Lorentz-Berthelot mixing rules [63], and σ_{CNT}=0.34 nm and ε_{CNT}/k_B=28 K the values usually accepted and applied for carbon atoms in graphite [64]. The LJ potential parameters for the 5-site model were adjusted by Severin and Tildesley considering methane molecule over graphite plane [56]. Comparision of the two interaction models of the methane molecules is presented in Figure 1. Both models of the CH_4 molecule describe interaction of methane molecule with a carbon atom of nanotube very similarly. However, interactions betwen the methane molecules are slightly different, especially for intermediate distances. In the MD simulations orientations of the methane molecules modelled by 5 interaction centres are described by quaternions. For the highest density of methane randomly oriented CH_4 molecules are placed in the fcc lattice nodes inside the CNT and small displacements from the crystalline positions are applied. Translational and angular velocities are chosen randomly and they are scaled to be consistent with the required temperature. Periodic boundary conditions along the CNT axis, together with the minimum image convention and spherical truncation of potential with cut-off radius r_c (see Table 2) are applied to the centres of mass of the molecules. To obtain lower densities part of the methane molecules are removed.

The Newtonian and orientational equations of motions are solved with the six- and five-value predictor-corrector integration scheme [63], respectively. The MD simulations are carried out in the canonical ensemble (NVT) at temperature T=293 K. At the beginning the system is far from the equilibrium state and distances between the interacting sites may be very small. Therefore, in the first stage (10000 steps) of each simulation the equations of motion are solved with a very short time step of about $0.15\cdot10^{-7}$ fs and after each 400 steps the time interval is doubled until it reaches the maximum value of 0.5 fs, which was applied through out the following 5000 time steps and in the next simulation stages. In the first two

stages we used the velocity scaling when deviation of the instantaneous temperature from the required one is larger than 3K. Then, 100000 time steps were performed to allow the system to achieve equilibrium configuration. Afterwards, the MD production runs were performed, where the configurations of the methane molecules, i.e. positions, orientations, and velocities are recorded. Simulation length of each MD production run depends on the density of methane molecules inside the CNT (see Table 1). In the last two stages temperature is generally maintained by the constraint method [63]. For the 5-site model the translational and rotational kinetic energies are constrained separately, and the equations of motions are folowing:

$$\frac{d}{dt}\mathbf{p}_i = \mathbf{F}_i - \xi_T \mathbf{p}_i, \qquad \xi_T = \frac{\sum_{i=1}^{N} \mathbf{F}_i \cdot \mathbf{p}_i}{\sum_{i=1}^{N} \mathbf{p}_i \cdot \mathbf{p}_i}, \tag{1}$$

$$\hat{I}^M \frac{d}{dt}\boldsymbol{\omega}_i^M = \mathbf{G}_i^M + \left[\boldsymbol{\omega}_i^M \times \left(\hat{I}^M \boldsymbol{\omega}_i^M\right)\right] - \xi_R \hat{I}^M \boldsymbol{\omega}_i^M, \qquad \xi_R = \frac{\sum_{i=1}^{N} \mathbf{G}_i^M \cdot \boldsymbol{\omega}_i^M}{\sum_{i=1}^{N} \left(\boldsymbol{\omega}_i^M\right)^T \hat{I}^M \boldsymbol{\omega}_i^M}. \tag{2}$$

In the above equations $\mathbf{p}_i$ and $\boldsymbol{\omega}_i$ are momentum and angular velocity of the ith molecule, respectively. $\mathbf{F}_i$ and $\mathbf{G}_i$ indicate force and torque, respectively, acting on the ith molecule. $\hat{I}$ is the tensor of inertia moment, ξ_T and ξ_R are dumping constants that fix the translational and rotational temperature, respectively, and the superscript M indicates a quantity in the molecular system. It must be noted that in the constraint method temperature tends to drift from its initial value [63]. Therefore, when the system temperature deviates from the required value by more than 3K the velocity scaling was applied. It must be noted that the velocity scaling is related to the constrained method, and for the leapfrog algorithm this method reduces to simple scaling of the velocities [65]. In the presented simulations the velocity scaling make small corrections of temperature. It was needed for the translational motion only and it was used once per about 10000 time steps for the highest density and 1000 time steps for the lowest one. To verify this approach some simulations were performed in the microcanonical ensemble (NVE), and their results for higher densities are in accordance with results of the NVT simulations described above, but for low densities temperature fluctuations are very high, up to 90K for the smallest system.

Structure of methane in CNT is characterized by a distribution of the CH_4 centres of mass across the CNT calculated as follows

$$\rho^R(r) = \frac{\langle N^R(r, r+\Delta r)\rangle}{Nd\Gamma}, \tag{3}$$

where $N^R(r,r+\Delta r)$ means number of molecules in a cylindrical shell with inner and outer radii r and $r+\Delta r$ (Δr=0.01 nm), respectively, and length L_z, $d\Gamma$ is the shell volume and angular brackets indicate averaging over time and the MD simulation runs. To investigate orientations of the methane molecules from the contact layer we calculate distribution of angles between C-H bonds and the normal to the CNT surface. The angle distribution is defined by

$$\rho^\varphi(\phi) = \frac{\langle N^\varphi(\phi, \phi+\Delta\phi)\rangle}{4N_C}, \tag{4}$$

where $N^\varphi(\phi,\phi+\Delta\phi)$ is number of the C-H bonds, whose angle with respect to the normal to the CNT surface is in the interval $(\phi,\phi+\Delta\phi)$ with $\Delta\phi$=1°, and N_C is number of the CH_4 molecules which were taken into account. The angle is defined as follows

$$\phi = \arccos\left[\frac{\mathbf{n}\cdot(\mathbf{r}_H - \mathbf{r}_C)}{|\mathbf{n}||\mathbf{r}_H - \mathbf{r}_C|}\right], \tag{5}$$

where $\mathbf{r}_H$ and $\mathbf{r}_C$ describe positions of the hydrogen atom and carbon one, respectively, in the CH_4 molecule, and the surface normal $\mathbf{n} = (x_C, y_C, 0)/\sqrt{(x_C^2 + y_C^2)}$ lays in the plane perpendicular to the pore axis and it is defined by coordinates of the carbon atom in the methane molecule.

To study dynamics of the systems we estimate self-diffusion coefficient, and two methods have been used to calculate the coefficient: one resulting from the linear response theory and the fluctuation-dissipation theorem, and the other from the Einstein formula [63]. For motion parallel to the pore axis the diffusion coefficient is defined by the following equations:

$$D = \int_0^\infty \langle v_z(t) v_z(0)\rangle dt, \tag{6}$$

$$D = \lim_{t\to\infty} \frac{1}{2t}\langle (z(t) - z(0))^2\rangle \tag{7}$$

where $v_z(t)$ and $z(t)$ are components of the velocity and position of the centre of mass of methane molecule at time t, respectively. In Equations (6) and (7) angular brackets mean averaging over molecules, the initial time and MD simulation runs, and the correlation functions appearing in those equations are calculated up to half of the MD simulation length. For long times the velocity autocorrelation functions approach zero, and the integral in Equation (6) is calculated for the whole time range. The mean-squared displacement (MSD) function change linearly with time except short times where ballistic motion is observed, and using Equation (7) to calculate the diffusion coefficient about 10% of the initial data in the MSD functions were ignored.

3. Results and Discussion

The distributions of methane across the CNT are similar for two models of methane molecule, and in Figure 2 we show the results of methane for the 5-site model only. For low densities methane form monolayer, with thickness of about 0.25 nm, near the nanotube wall, and maximum of the monolayer peak is observed at about 0.65 nm. For higher densities some of the particles are localised in the inner part of the CNT. The distribution peaks for the rigid CNT are narrower than those for the flexible one, when thermal fluctuations of the wall atoms make roughness of the surface more evident and increase frequency of collisions of methane molecules with nanotube atoms. The layered structure of methane in CNT is also demonstrated in Figure 3, which presents projection of positions of the methane molecules on the plane perpendicular to the CNT axis for selected loadings of methane.

Additional information about structure of methane in the CNT is given by the angle distribution of bonds of the CH_4 molecules from the contact layer $\rho^{\varphi}(\phi)$. The distributions presented in Figure 4 were calculated for molecules for which a distance from the CNT axis is larger than 0.65 nm, i.e. the position of the monolayer peak maximum (compare Figure 2). For all densities the functions are similar, and hence in Figure 4 we show results for two systems only: the highest loading of methane considered here and the lowest one. In the functions there are two broad peaks: the first peak with maximum at about 65° and the other one with maximum at about 160°, which is approximately three times weaker than the first one. The distribution functions suggest that a tripod orientation of the methane molecule with respect to the CNT surface is preferred. For both models of the CNT the angle distributions are almost the same. This observation indicates weak impact of the CNT flexibility on orientation of the methane molecules in the vicinity of the CNT wall. Similar

shapes of the distribution function were observed considering thicker layer when distance of a molecule from the CNT axis is larger than 0.5 nm, but the peaks of the distribution functions are less pronounced than those presented in Figure 4. These results suggest that the tripod orientation is characteristic for molecules near the CNT wall, but molecules localised further from the nanotube surface do not show any preferred orientation. One must note that for ideal tripod orientation the angles, which C-H bonds form with the normal to the CNT surface are following: one of 180° and three ones of 70.5°, and such orientation is suggested by studies of methane adsorbed on a graphite surface using the classical MD simulation [47,54] and DFT method [49,55]. In other words the methane molecules in CNT are tilted with respect to the ideal tripod orientation. The tilted tripod position of a molecule lying nearby the CNT surface is confirmed by energy minimization of single methane molecule in the CNT. The conjugate gradient method gave minimum of the interaction energy for the CH_4 molecule localised 0.337 nm above a carbon atom in the nanotube with the tripod legs oriented toward the centres of the three adjacent carbon hexagons as it is shown in Figure 5. This distance is found to be similar to results predicted for methane molecules inside the (10,10) CNT [24,25] and the (10,0) one [25]. The observed distance between the methane molecule and the nanotube surface is in good agreement with the experimental results for methane adsorbed on a graphite sheet, which changes from 0.33 nm [40] when methane molecules form an adlayer with the $\sqrt{3}\times\sqrt{3}$ structure [41] to 0.345 nm estimated at low coverage [48]. The energy minimalization gives also angles between the methane bonds and the surface normal, and they are following: for $C\text{-}H_1$ it is 178.3° , for $C\text{-}H_3$ 72.2° and for $C\text{-}H_2$ and $C\text{-}H_4$ 69.7° (see Figure 5). The angles indicate that the tilt appears in the plane perpendicular to the nanotube axis, and one may suspect that the tilt results from curvature of the nanotube. To confirm this suggestion similar calculations were performed for single CH_4 molecule in the (10,10) CNT and (60,60) one with diameters 1.354 nm and 8.124 nm, respectively. For the small nanotube an angle between the $C\text{-}H_1$ bond and surface normal is 175.4°, which is smaller than that for the (15,15) CNT, whereas for the large CNT the angle is 179.9° and this value is very close to that for graphene sheet.

The diffusion coefficient values for CH_4 in the rigid CNT and flexible one for both methane models are presented in Figure 6. In all cases under consideration the diffusion coefficients obtained from Equations (6) and (7) are very similar, and hence we show only results obtained from velocity autocorrelation function, and the coefficient errors were estimated using results obtained from the consecutive MD simulation runs. The value

of diffusion coefficient for both methane models drops dramatically with density due to the increase of frequency of intermolecular collisions. This observation is in accordance with previous simulations [15-17,21,23] and it is due to dominated methane-methane collisions over the methane-carbon ones. However, for low densities the values of the diffusion coefficient for the 1-site model are higher than those for the 5-site one. In other words, the realistic model of the methane molecule becomes important at low densities. Moreover, comparing results presented in Figure 6(a) and Figure 6(b) one may conclude that the diffusivity of methane molecules in a flexible nanotube differ very little from that for a rigid one suggesting that the vibration of the nanotube carbon atoms which interact through the REBO potential has a little influence on translational motion of methane molecules.

To compare the diffusion coefficients obtained here with accessible data [15,16,21] we estimated adsorptive pressures of methane in the (15,15) CNT using isoterms reported by Nicholson [66]. Dependence of the diffusion coefficient on pressure obtained by Jakobtorweihen et al. [15,16] and Chen et al. [21] together with our results when the methane molecule is represented by one LJ interaction centre are shown in Fig. 7.
In all cases diffusion coefficient depends on pressure similarly, however its values obtained here are slightly smaller than those published earlier [15, 16, 21] that may be result of different simulation methods. Moreover, it is seen that our smallest system 5/4L is out of the low-density region for which the earlier studies [15, 16, 21] show faster translational motion of methane in the rigid CNT than that in the flexible one. In other words, our results for the REBO potential, support a conclusion of the previous works that impact of the nanotube flexibility on methane behaviour in the CNT is small at high and intermediate densities.

4. Conclusions

Properties of methane in CNT are studied using the MD simulation method. The results obtained for methane densities considered here, i.e. for states from the dense gas phase to the liquid one, show that impact of the CNT flexibility, introduced by the REBO interaction potential, on translational motion and structure of methane molecules is weak. Values of the diffusion coefficient of methane molecules in the rigid CNT and flexible one are almost the same. Similarly, shapes of the distribution functions of angles between the C-H

bonds in the methane molecule and the CNT surface normal are alike for both nanotubes. A slight difference is observed in density profiles across the CNT. For both models of CNT one observes layered structure of methane by nanotube wall, but methane molecules in the rigid CNT show better localisation near the nanotube wall than those in the flexible CNT.

Distribution of methane molecules in the CNT is almost independent on the methane molecule model. The simulation results show that the diffusion coefficients for the two models of CH_4 considered here are comparable only for higher densities, whereas for low densities atomic strucuture of methane molecule leads to reduction of the diffusion coefficient. One may conclude that approximation of the methane molecules by spherical super-atoms is reasonable for higher densities. Moreover, one may suspect that atomic structure of the molecule may be important at temperatures lower than that considered here.

Distribution of the methane molecule orientation suggests tilted tripod position of the molecules from monolayer with respect to the CNT. This conclusion is confirmed by the energy minimization of one CH_4 molecule in the CNTs, and the tilt of the molecule results from curvature of the nanotube.

References

[1] B.J. Hinds, N. Chopra, T. Rantell, R. Andrews, V. Gavalas, and L.G. Bachas, Science **303**, 62 (2004).

[2] D.W. Deamer and M. Akeson, Trends Biotechnol. **18**, 147 (2000).

[3] M.-H. Hong, K.H. Kim, J. Bae, and W. Jhe, Appl. Phys. Lett. **77**, 2604 (2000).

[4] A. Kleinhammes, S.-H. Mao, X.-J. Yang, X.-P. Tang, H. Shimoda, J. P. Lu, O. Zhou, and Y. Wu, Phys. Rev. B **68**, 075418 (2003).

[5] F.J.A.L. Cruz and J.P.B. Mota, Phys. Rev. B **79**, 165426 (2009).

[6] M. Bienfait, B. Asmussen, M. Johnson, and P. Zeppenfeld, Surface Science **460**, 243 (2000).

[7] E. Bekyarova, K. Murata, M. Yudasaka, D. Kasuya, S. Iijima, H. Tanaka, H. Kahoh, and K. Kaneko, J.Phys. Chem. B **107**, 20 (2003).

[8] D.S. Rawat, M.M. Calbi, and A.D. Migone, J. Phys. Chem. C **111**, 12980 (2007).

[9] M.R. Johnson, S. Rols, P. Wass, M. Muris, M. Bienfait, P. Zeppenfeld, and N. Dupont-Pavlovsky, Chemical Physics **293**, 217 (2003).

[10] M.Muris, N.Dupont-Pavlovsky, M. Bienfait, and P. Zeppenfeld, Surf. Science **492**, 67 (2001).

[11] S. Talapatra and A.D. Migone, Phys. Rev. B **65**, 045416 (2002).

[12] M. Bienfait, P. Zeppenfeld, N. Dupont-Pavlovsky, M. Muris, M.R. Johnson, T. Wilson, M. DePies, and O.E. Vilches, Phys. Rev. B **70**, 035410 (2004).

[13] M. Muris, N. Dufau, M. Bienfait, N. Dupont-Pavlovsky, Y. Grillet, and J.P. Palmari, Langmuir **16**, 7019 (2000).

[14] S. Jiang, C.L. Rhykerd, and K.E. Gubbins, Mol. Phys. **l79**, 373 (1993).

[15] S. Jakobtorweihen, M. G. Verbeek, C.P. Lowe, F.J. Keil, and B. Smit, Phys. Rev. Lett. **95**, 044501 (2005).

[16] S. Jakobtorweihen, C.P. Lowe, F.J. Keil, and B. Smit, J. Chem. Phys. **124**, 154706 (2006).

[17] A.I. Skoulidas, D.M. Ackerman, J.K. Johnson, and D.S. Sholl, Phys. Rev. Lett. **89**, 185901 (2002).

[18] Z. Mao and S.B. Sinnott, J. Phys. Chem. B **104**, 4618 (2000).

[19] D. Cao and J. Wu, Langumir **20**, 3759 (2004).

[20] V.P. Sokhan, D. Nicholson, and N. Quirke, J. Chem. Phys. **117**, 8531 (2002).

[21] H. Chen, J.K. Johnson, and D.S. Sholl, J. Phys. Chem. B **110**, 1971 (2006).

[22] C. Rhykerd, Z. Tan, L.A. Pozhar, and K.E. Gubbins, J. Chem. Soc. Faraday Trans. **87**, 2011 (1991).

[23] S. Jakobtorweihen, F.J. Keil, and B. Smit, J. Phys. Chem. B **110**, 16332 (2006).

[24] S. Shokri, R. Mohammadikhah, H. Abolghasemi, A. Mohebbi , H. Hashemipour, M. Ahmadi-Marvast, and Sh. Jafari Nejad, Int. J. of Chem. Eng. and Applications **1**, 63 (2010).

[25] K.-H. Lee and S.B. Sinnott, J. Phys. Chem. B **108**, 9861 (2004).

[26] S.Y. Bhide and S. Yashonath, J. Chem. Phys. **116**, 2175 (2002).

[27] Z. Mao, A.Garg, and S.B. Sinnott, Nanotechnology **10**, 273 (1999).

[28] D. Cao, X. Zhang, J. Chen, W. Wang, and J.Yun, J. Phys. Chem. B **107**, 13286 (2003).

[29] P. Kowalczyk, H. Tanaka, K. Kaneko, A.P. Terzyk, and D.D. Do, Langmuir **21**, 5639 (2005).

[30] B.-H. Kim, G-H. Kum, and Y.-G. Seo, Korean. J. Chem. Eng. **20**, 104 (2003).

[31] P. Kowalczyk, L. Solarz, D.D. Do, A. Samborski, and J.M.D. MacElroy, Langmuir **22**, 9035 (2006).

[32] M.R. LaBrosse, W. Shi, and J.K. Johnson, Langmuir **24**, 9430 (2008).

[33] M.D. Ganji, M. Asghary, and A.A. Najafi, Commun. Theor. Phys. (China) **53,** 987 (2010).

[34] J. Zhao, A. Buldum, J. Han, and J.P. Lu , Nanotechnology **13**, 195 (2002).

[35] H. Tanaka , M. El-Merraoui, W.A. Steele, and K. Kaneko, Chem. Phys. Lett. **352**, 334 (2002).

[36] A.G. Albesa, E.A. Fertitta, and J.L. Vicente, Langmuir **26**, 786 (2010).

[37] B.K. Agrawal, S. Agrawal, S. Singh, and R. Srivastava, J. Phys.: Condens. Matter **18**, 4649 (2006).

[38] P.A. Denis, Chem. Phys. **353**, 79 (2008).

[39] A. Ricca and C.W. Bauschlicher Jr., Chem. Phys. **324**, 455 (2006).

[40] G. Bomchil, A. Huller, T. Rayment, S.J. Roser, M.V. Smalley, R.K. Thomas, and J.W.White, Phil. Trans. R. Soc. Lond. B **290**, 537 (1980).

[41] K. Knorr, Phys. Rep. **214**, 113 (1992) .

[42] J.P. Coulomb, M. Bienfait, and P. Thorel, Phys. Rev. Lett. **42**, 733 (1979).

[43] J.H. Quateman and M.Bretz, Phys. Rev. Let. **49**, 20 (1982).

[44] H.K. Kim, Q.M. Zhang, and M.H.W. Chan, Phys. Rev. B **34**, 4699 (1986).

[45] M.J. Lysek, M.A. LaMadrid, P.K. Day, and D.L. Goodstein, Phys. Rev. B **47**, 12 (1993).

[46] R.P. Humes, M.V. Smalley, T. Rayment, and R.K.T. Can, J. Chem. **66**, 557 (1988).

[47] L.W. Bruch, J. Chem. Phys. **87**, 5518 (1987).

[48] G. Vidali, G. Ihm, H-Y. Kim, and M.W. Cole, Surf. Sci. Rep. **12**, 135 (1991).

[49] S. Yang, L. Ouyang, J.M. Phillips, and W.Y. Ching, Phys. Rev. B **73**, 165407 (2006).

[50] J. M. Phillips, Phys. Rev. B **29**, 5865 (1984).

[51] K.A. Hunzicker and J.M. Phillips, Phys. Rev. B **34**, 8843 (1986).

[52] J.M. Phillips, Phys. Rev. B **34**, 2823 (1986).

[53] H.-Y. Kim and W.A. Steele, Phys. Rev. B **45**, 11 (1992).

[54] J.M. Phillips and M.D. Hammerbacher, Phys. Rev. B **29**, 5859 (1984).

[55] M. Rubes, J. Kysilka, P. Nachtigall, and O. Bludsky, Phys. Chem. Chem. Phys **12**, 6438 (2010).

[56] E.S. Severin and D.J. Tildesley, Mol. Phys. **41**, 1401 (1980).

[57] D.W. Brenner, O.A. Shenderova, J.A. Harrison, S.J. Stuart, N. Ni, and S.B. Sinnott, J. Phys.: Condes. Matter **14**, 783 (2002).

[58] A. Bródka, J. Kołoczek, and A. Burian, J. Nanosc. Nanotechn. **7**, 1505 (2007).

[59] B.I. Yakobson, C.J. Brabec, and J. Bernholc, Phys. Rev. Lett. **76**, 2511 (1996).

[60] S.B. Sinnott, O.A. Shenderova, C.T. White, and D.W. Brenner, Carbon **36**, 1 (1998).

[61] Ł. Hawełek, J. Kołoczek, A. Bródka, J.C. Dore, V. Honkimäki, A. Fonseca, and A. Burian, Phil. Mag. **87**, 4973 (2007).

[62] A. Bródka, T.W. Zerda, and A. Burian, Diam. Rel. Mat. **15**, 1818 (2006).

[63] M.P. Allen and D.J. Tildesley, "Computer Simulation Of Liquids", (Clarendon Press, Oxford, 1989).

[64] L.A. Girifalco, M. Hodak, and R.S. Lee, Phys. Rev. B **62**, 13104 (2000).

[65] D. Brown, J.H.R. Clarke, Mol. Phys. **51,** 1243 (1984).

[66] D. Nicholson, Mol. Phys. **100**, 2151 (2002).

Table 1. Systems under consideration and lengths of the MD production runs.

System symbol (number of CH_4 molecules/ the CNT length)	240/L	180/L	120/L	60/L	60/2L	60/4L	40/4L	20/4L	10/4L	5/4L
MD simulation length [ps]	50	50	50	50	50	50	300	400	500	600
Number of simulation runs	4	4	4	4	4	4	6	8	10	12

Table 2. Parameters of the LJ interactions.

	5-site model			1-site model		
INTERACTIONS	ε / k_B [K]	σ [nm]	r_c [nm]	ε / k_B [K]	σ [nm]	r_c [nm]
CH_4- CH_4			1.06	148.1	0.381	1.00
C_{MOL}-C_{MOL}	51.198	0.335				
C_{MOL}-H_{MOL}	23.798	0.299				
H_{MOL}-H_{MOL}	4.87	0.261				
CNT- CH_4			1.04	64.4	0.361	0.95
C_{CNT}-C_{MOL}	47.68	0.330				
C_{CNT}-H_{MOL}	17.00	0.298				

Figure captions

Figure 1. The LJ potential for 1-site model and 5-site one averaged over orientations of the methane molecules.

Figure 2. Density distribution of methane molecules (5-site model) across the CNT for (a) rigid and (b) flexible nanotube.

Figure 3. Projection of centres of methane molecule (5-site model) in the rigid CNT on a plane perpendicular to the nanotube axis for the systems marked (see Table1).

Figure 4. Distribution of angles between C-H bonds of methane molecule and the normal to the CNT wall for (a) rigid and (b) flexible nanotube.

Figure 5. Position of the CH_4 molecule with respect to the carbon atoms of the nanotube. Grey circles represent the hydrogen atoms, black circles the carbon ones. Solid line is parallel to the nanotube axis.

Figure 6. Diffusion coefficient D as a function of linear density of methane, λ, for (a) rigid and (b) flexible nanotube.

Figure 7. . Comparision of diffusion coefficients obtained here (stars) with data reported in [15,16,21].